Eur. Phys. J. A **25**, s01, 623–628 (2005)
DOI: 10.1140/epjad/i2005-06-103-4

EPJ A direct
electronic only

Amazing developments in nuclear astrophysics

A.E. Champagne[a]

The University of North Carolina at Chapel Hill, Chapel Hill, NC 27599-3255, USA, and Triangle Universities Nuclear Laboratory, Durham, NC 27708-0308, USA

Received: 12 January 2005 /
Published online: 2 June 2005 –

Abstract. The time since ENAM '01 is short by astrophysical standards, but this period has seen some exciting progress in the area of experimental nuclear astrophysics. New results have been obtained from facilities both large and small, with stable and exotic beams. In the process, we have learned a great deal about stellar structure and evolution. This talk highlights a few of many notable results obtained since ENAM '01 and will attempt to place them into an astrophysical context. In the process, it may be possible to see where the field is heading and what we might anticipate over the next three years.

PACS. 26.20.+f Hydrostatic stellar nucleosynthesis – 26.30.+k Nucleosynthesis in novae, supernovae and other explosive environments – 97.10.Cv Stellar structure, interiors, evolution, nucleosynthesis, ages

1 Introduction

Progress in nuclear astrophysics often comes at a measured pace. In many instances a number of nuclear processes may give rise to a particular stellar observable and a systematic approach is needed to gain insight into the underlying astrophysics. On the other hand, there are certainly cases where a single reaction or decay can say a great deal about a particular issue in astrophysics. Two obvious examples of this latter situation are the ^{7}Be(p,γ)^{8}B reaction (and the solar neutrino problem), and ^{12}C(α,γ)^{16}O (and the evolution of massive stars). Although both reactions have received a great deal of attention in the past 3 years, neither will be featured here. This is not to say that they are unimportant —indeed, they remain as critical challenges for the field. Both will be "solved" by an accumulation of experimental results and it is too early to declare victory on either front. In contrast, the last 3 years have seen striking progress in other areas of nuclear astrophysics, which will be the main focus of attention in this review.

2 ^{14}N(p, γ)^{15}O and the age of the galaxy

One way of estimating the age of the galaxy is by determining the ages of its oldest stellar populations —the globular clusters. Presently, the best understood method for determining the age of a cluster is by locating the "main sequence turnoff" on a color-magnitude plot of the stars in a cluster. This represents the transition point between core hydrogen burning that characterizes the main sequence and shell hydrogen burning on the red giant branch. The turnoff luminosity has a well-defined relationship with the age of the population of stars.

The primary uncertainty in this procedure involves determining the distance to the cluster (and hence the absolute luminosity), but there is some confidence that distance determinations will become more reliable. There are also uncertainties involved with the chemical composition of the cluster, model parameters (such as opacity, convection, etc.) and one nuclear reaction, ^{14}N(p,γ)^{15}O [1]. This latter source of uncertainty may seem surprising, since the stars of interest are low-mass stars that spend most of their lives generating energy via the pp-chains. However, the core temperature increases during the main sequence stage to the point where the CN-cycle becomes the dominant source of energy near the turnoff point. The power generated by the CN-cycle is governed by the rate of the slowest reaction, namely ^{14}N(p,γ)^{15}O.

The previously accepted rate for the ^{14}N(p,γ)^{15}O reaction is based on measurements by Schröder *et al.* [2] (hereafter Sch87), which showed that a subthreshold resonance made a significant contribution to the total cross-section. This assertion was questioned in several subsequent studies [3,4,5,6,7] and recently, two independent experiments have been performed to directly measure the low energy part of the ^{14}N(p,γ)^{15}O cross-section. One was carried out at the (underground) LUNA facility at the Gran Sasso Laboratory [8], and the other at the LENA facility, which is part of TUNL [9]. The astrophysical S-factors for the 3 main transitions are shown in fig. 1 and the results of the 2 experiments are in excellent agreement.

[a] Conference presenter; e-mail: `aec@tunl.duke.edu`

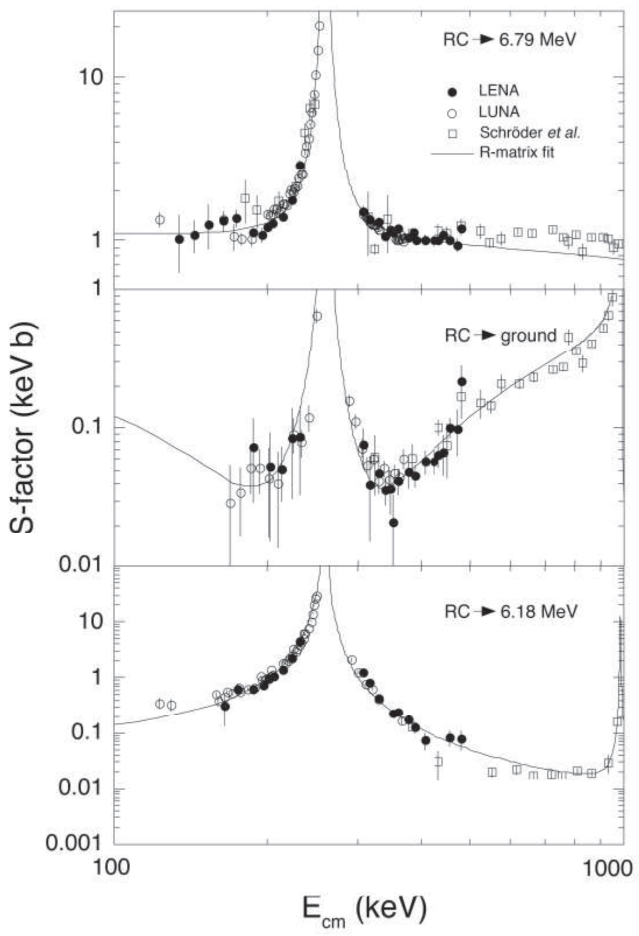

Fig. 1. S-factors for the major transitions in $^{14}N(p,\gamma)^{15}O$. Here, RC denotes radiative capture. The results of the LUNA [8] and LENA [9] measurements are denoted by the open and solid circles, respectively. The data from Sch87, corrected for summing and with yield data removed [10] are shown as open squares. The solid lines are R-matrix fits to the combined data set [10].

The combined data determine the S-factor at zero energy to about 10% [10] and for temperatures less than about 10^8 K, the total S-factor (and reaction rate) is approximately 50% of the previously recommended value [11]. This temperature range includes main sequence and red giant stars. In the case of main sequence models, the reduction in the power generated by the CN-cycle produces compensating structural changes in the core. In particular, the core becomes slightly cooler, but larger and more dense. This moves the star to higher effective temperature and luminosity on the color-magnitude diagram. In order to match a turnoff luminosity calculated with the old rate, a calculation with the revised rate requires increasing the age of the star (or reducing its mass), which moves it to lower effective temperature and luminosity. In other words, the ages derived for globular clusters must increase. Detailed calculations show an increase of 0.7–1 Gy [12], which moves the best-fit age (as defined by [1]) of globular clusters to 13.4 Gy. This is still consistent with the WMAP age of the Universe (13.7 Gy [13]), but implies that globular clusters formed soon after the first stars in the Universe.

3 Novae and X-ray bursts

As their names suggest, novae and Type I X-ray bursts are observationally quite different, but share a similar underlying mechanism. Both occur in binary systems and are triggered by mass transfer from a main-sequence or giant star onto a companion white dwarf (nova) or neutron star (X-ray burst). Once the accreted mass reaches a critical temperature and density, it ignites under degenerate conditions and a thermonuclear runaway ensues. The conditions governing each class of outburst are quite different. Novae reach peak temperatures of less than 4×10^8 K and densities of 10^3–10^4 g/cm^3 whereas X-ray bursts occur at much higher temperatures ($> 10^9$ K) and densities ($> 10^5$ g/cm^3). A description of either event must take into account the central role of convection and other uncertain, but critical aspects such as the mass transfer rate. However, since both explosions are driven by nuclear processes, nuclear information can be used to decipher the observational record.

3.1 γ-ray production in novae

One nucleus of interest for novae is ^{18}F. The radioactive decay of ^{18}F may be an important energy source during the early part of the visible outburst and the ensuing γ-emission may someday be detected. The net abundance of ^{18}F is determined by the competition between production and destruction reactions and the major contributor to the latter is the $^{18}F(p,\alpha)^{15}O$ reaction. This reaction has been measured directly [14] down to energies corresponding to a resonance at a center-of-mass energy of $E_{cm} = 330$ keV, which is near the upper end of the relevant energy range. For states at lower energies, the proton width would be much less than the alpha and therefore the resonance strength is determined by the proton width.

Recently, groups at Louvain la Neuve [15] and at Oak Ridge [16] have used the $d(^{18}F,p)^{19}F$ reaction to locate the analogs of potential $^{18}F + p$ resonances and to measure their neutron spectroscopic factors. Both studies used the assumption of isospin symmetry to determine the proton spectroscopic factor and thus the proton width for the corresponding state in ^{19}Ne. The 2 results differ in significant details, particularly in the question of whether there is a resonance at $E_{cm} = 38$ keV. However, the respective reaction rates agree within uncertainties (fig. 2). If the rate is actually near the lower end of the allowed range, then the net abundance of ^{18}F would be 3–5 times previous predictions. Clearly, further work to better define the reaction rate would be valuable.

Another target of opportunity for γ-ray astronomy is ^{22}Na. In novae and X-ray bursts, ^{22}Na is produced via the

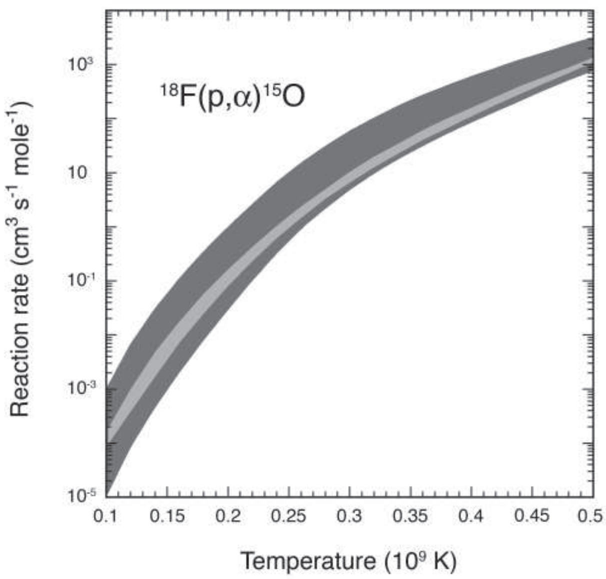

Fig. 2. Reaction rate for the $^{18}F(p,\alpha)^{15}O$ reaction. The dark shaded region is the result from the Louvain la Neuve experiment [15] and the lighter band is from the Oak Ridge experiment [16].

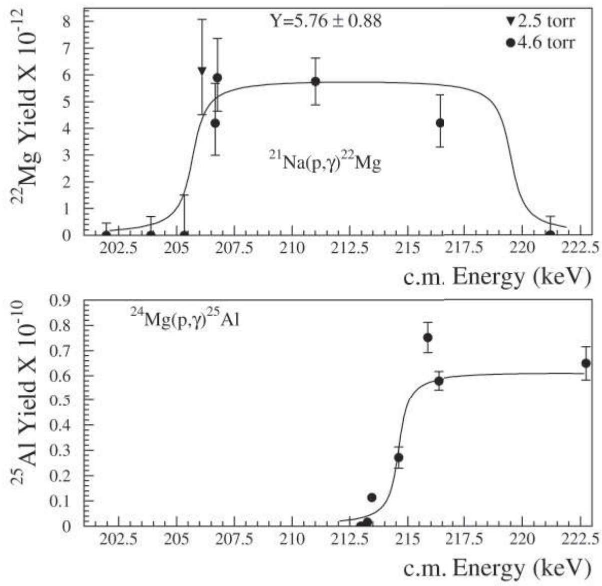

Fig. 3. The upper panel shows the thick target yield data for the $^{21}Na(p,\gamma)^{22}Mg$ reaction, obtained with the ISAC facility and DRAGON recoil separator. The solid line is the calculated yield for (gas) target thickness of 4.6 torr. The lower panel is the yield of the 214 keV resonance in the $^{24}Mg(p,\gamma)^{25}Al$, which was used for beam energy calibration. All errors are statistical. *Reprinted figure with permission from S. Bishop et al., Phys. Rev. Lett.* ***90****, 162501 (2003). Copyright 2003 by the American Physical Society.*

sequence

$$^{20}\mathrm{Ne}(\mathrm{p},\gamma)^{21}\mathrm{Na}(\beta^+)^{21}\mathrm{Ne}(\mathrm{p},\gamma)^{22}\mathrm{Na}, \qquad (1)$$

or by

$$^{20}\mathrm{Ne}(\mathrm{p},\gamma)^{21}\mathrm{Na}(\mathrm{p},\gamma)^{22}\mathrm{Mg}(\beta^+)^{22}\mathrm{Na}. \qquad (2)$$

Because of the rather slow β^+-decay of ^{21}Na ($T_{1/2}$ = 22.5 s), these sets of reactions may occur on quite different time scales and therefore at different phases in the explosion. It is believed that the reaction flow should favor the former sequence if significant amounts of ^{22}Na are to be produced [17]. However, uncertainties in the rate of the $^{21}Na(p,\gamma)^{22}Mg$ reaction lead to large uncertainties in the predicted abundance [18] of ^{22}Na.

The rate of the $^{21}Na(p,\gamma)^{22}Mg$ reaction depends upon the strengths of a relatively small number of isolated, narrow resonances. Determining the properties of these resonances indirectly has proven to be difficult because it has not been possible to make a firm connection to the comparatively well studied analog states in ^{22}Ne. This situation has changed dramatically with the results of *direct* (p,γ) measurements using the ISAC facility at TRIUMF [19,20]. A yield curve for the lowest resonance (at E_{cm} = 206 keV) is shown in fig. 3. This work determines the reaction rate to an accuracy normally associated with stable beams and targets, and shows that the $^{21}Na(p,\gamma)$ path is favored in ONe novae. The result is that ^{22}Na is produced earlier in the explosion, when the temperature is higher and when it is more readily destroyed [20]. This reduces the final yield of ^{22}Na and lowers the predicted γ-ray flux. Unfortunately, the prospects for observing γ-emission from ^{22}Na are correspondingly reduced.

3.2 Impedance effects in the rp-process

In Type I X-ray bursts, nucleosynthesis can proceed via the αp- and rp-processes beyond iron and perhaps to the Sn-Te region [21]. High temperatures and densities ensure that most of these reactions are extremely fast and therefore, their actual rates are relatively unimportant. What is important is knowing where and how the reaction flow is impeded. This affects the energy budget and the light curve, both of which can be observed [22].

One of these waiting points is expected to occur at ^{68}Se (as shown in fig. 4). Because ^{69}Br is most likely unbound, the rp-flow must pause until ^{68}Se either β^+-decays (with a laboratory half life of 35.5 s) or undergoes a 2p-capture to ^{70}Kr. The 2p-capture is actually a sequential process: $^{68}Se(p,\gamma)^{69}Br(p)^{68}Se$ produces a small equilibrium abundance of ^{69}Br, which can then undergo a subsequent proton capture. The rate for converting ^{68}Se into ^{69}Br depends in part on the mass difference between ^{68}Se+p and ^{69}Br, which enters exponentially into the rate equation [23,24]. Recently, the mass of ^{68}Se was measured to very high precision (1 part in 2854) using the Canadian Penning Trap at Argonne National Laboratory [25]. The stellar half life of ^{68}Se was then calculated using a theoretical value for the mass of ^{69}Br [26]. Under typical conditions, the rate for 2p-capture is much slower than that for β^+-decay and thus the reaction flow slows considerably. This finding was confirmed by another, independent measurement of the mass of ^{68}Se [27].

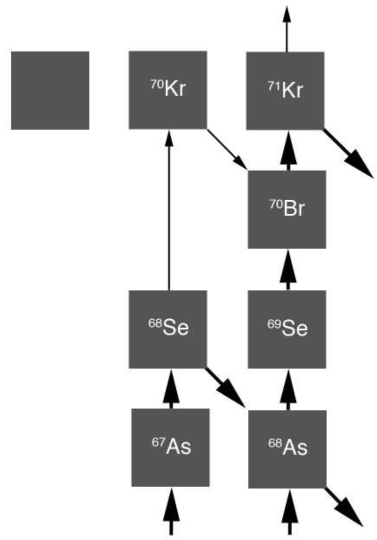

Fig. 4. The rp-process near ^{68}Se.

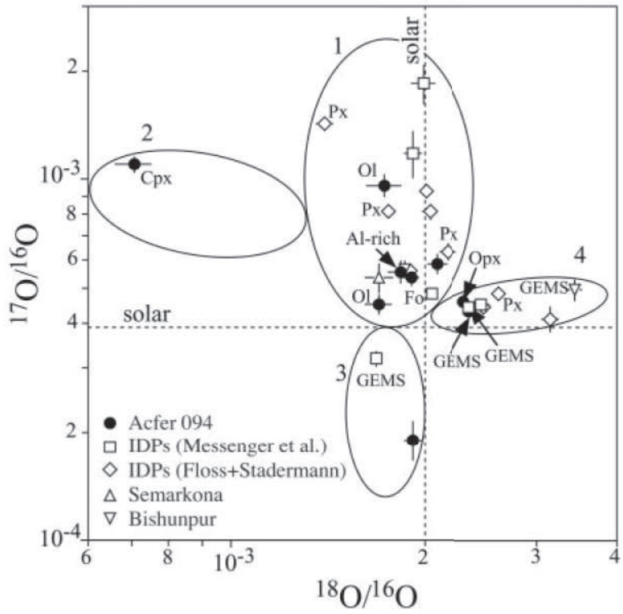

Fig. 5. Oxygen isotopic compositions (with 1-σ uncertainties) of presolar silicate grains from the meteorite Acfer 094 compared with those of silicates from various interplanetary dust particles (IDP) and from the ordinary chondrites Semarkona and Bishunpur (14, 15). The mineralogy of the grains is indicated: Clinopyroxene, Cpx; orthopyroxene, Opx; olivine, Ol; pyroxene, Px; forsterite, Fo. Also shown are four different groups of grains defined by the systematics of other oxide grains [31]. *Reprinted figure with permission from A.N. Nguyen and E. Zinner, Science **303**, 1496 (2004). Copyright (2004) AAAS.*

If the rp-process does slow down at ^{68}Se, then the energy generated at later times in the outburst will be reduced and more power will appear in the peak of the burst [22]. However, nuclear structure may change this picture. New work has shown that a shape isomer exists in a neighboring $N = Z$ nucleus, ^{72}Kr [28], which is manifested by a 0^+ first excited state. If a similar structure exists in ^{68}Se, then the first excited state could be efficiently populated by thermal excitations, which would lower the Q-value for 2p-capture and increase the phase space term in the β^+-decay rate. Either effect would speed the reaction flow through ^{68}Se. This situation also shows how progress in nuclear structure can become relevant for nucleosynthesis.

4 Presolar grains

Presolar grains are pieces of stars that can be brought into the laboratory and analyzed in great detail. Systematic studies reveal contributions from specific types of stars that can be identified based on their unique *isotopic* signatures (see, *e.g.* [29] for a recent review). In contrast, stellar spectroscopy is limited with few exceptions to *elemental* abundances. Although meteoritics is not a new field, the isolation and analysis of presolar grains is a fairly new development that has been driven by constant advances in technology. One challenge has been that most grains are sub-micron in size and thus could not be analyzed individually. However, it is now possible to do just this, which has lead to the discovery of presolar silicates [30]. Silicates are expected from a variety of sites, including young main-sequence stars and in oxygen-rich asymptotic giant branch stars. However, the Solar System itself is rich in silicates and until now it has been impossible to separate out a few presolar silicate grains amongst a comparatively vast number of solar silicates.

The nine grains that have been isolated thus far have oxygen isotopic ratios that are consistent with origin at some stage on the red giant branch (see fig. 5). One grain also shows the signature of stellar ^{26}Al (preserved as an anomalous abundance of ^{26}Mg). In addition to providing information about stars, these grains can be compared with silicates from other sources to provide information about the formation history of meteorites and conditions in the early Solar System.

5 Back to the future with the r-process

About half of the elements heavier than iron are formed under conditions of high temperature and neutron density in what is known as the r-process. Observations of very old stars in the halo of our galaxy show an r-process abundance pattern that looks quite similar to what is observed in the Solar System (see for example, the recent review by Truran *et al.* [32]). However, the abundances of radioactive Th and U are observed to fall below the relative solar abundance, which implies that the ages of these stars lie in the range 14 ± 3 Gy [33,34,35]. This assumes that the initial r-process abundance pattern can be calculated, despite the fact that it has not been possible to

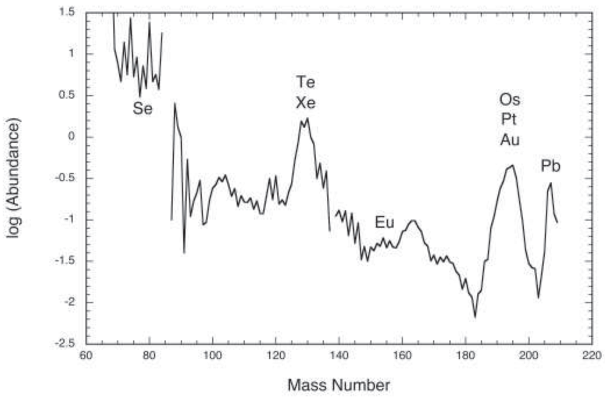

Fig. 6. Abundances of the r-process elements in the Solar System (from the data of ref. [36]).

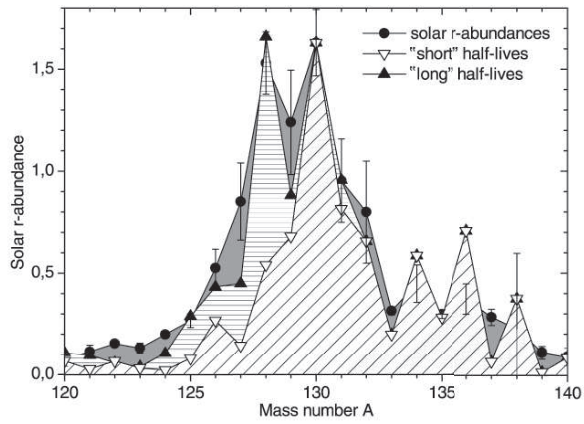

Fig. 7. Comparison of the Solar System r-process abundances in the $A \approx 130$ peak region with model predictions. Within the classical "waiting-point" concept, the "longer" half-lives concluded from new nuclear-structure information result in a better reproduction of the rising wing of the solar r-abundance peak. *Reprinted figure with permission from I. Dillmann et al., Phys. Rev. Lett.* ***91****, 162503 (2003). Copyright 2003 by the American Physical Society.*

establish the site of the r-process. So this look into the past points towards one of the frontier areas of the field.

Hints about the conditions governing the r-process are contained in the distribution of the r-process elements (shown in fig. 6). For example, the abundance peaks are the remnants of nuclei formed near closed neutron shells and well to the neutron-rich side of stability. A brief (and extremely simplified) picture is that the r-process occurs in supernovae, when the temperature and neutron density are high enough to produce an $(n,\gamma) \leftrightarrow (\gamma,n)$ equilibrium. This behavior links nuclei along a line of constant neutron separation energy, S_n, initially 10–40 neutrons away from stability. The flow to higher masses is slowed at the neutron magic numbers, where S_n drops and photodisintegration is favored. Steady flow is re-established only after several β-decays and so material accumulates at these waiting points. As the neutron density drops, β-decays move the entire abundance distribution toward higher S_n. Finally, the temperature and density will drop to the point where the β-flow reaches stability. Because the r-process occurs so far from stability, essentially all of the relevant nuclear physics input must be obtained from theory (for now)!

The abundance peaks shown in fig. 6 are end products of the waiting points at the closed neutron shells, and their locations and shapes are influenced by a number of factors such as β-decay rates [37,38], late n-captures [39], β-delayed n-decays, etc. Thus, they are of particular interest as diagnostics of the conditions and physics of the r-process. For example, it has been known for some time that the $N = 82$ and $N = 126$ shell splittings must be reduced in order to reproduce the $A \approx 130$ and $A \approx 195$ abundance peaks in detail [40]. There is experimental evidence for shell quenching in other mass regions, but at present it is possible to produce only a select few r-process nuclei.

One of these nuclei is ^{130}Cd, which is part of the $N = 82$ waiting point. The decay scheme of ^{130}Cd reveals several interesting features [41]. For example, the β-decay Q-value is higher than that predicted by mass models that include strong shell splittings. Several models that include shell quenching do a much better job of matching the experimental value. Also, a significant finding is that the energy of the 2QP, 1^+ GT state is substantially higher than expected. In order to reproduce this result using the shell model, the relevant 2-body matrix element for β-decay of ^{130}Cd must be reduced. If this is a global effect, then the predicted lifetimes of the $N = 82$ waiting-point nuclei will increase. The manifestation of this change is a broadening of the $A \approx 130$ abundance peak to lower masses (fig. 7), which does a much better job of reproducing the observed abundances without invoking any exotic post processing (for example, neutrino interactions).

6 Conclusion

This paper has described —in a superficial way— a number of interesting new results that span a range of topics from cosmology to stellar evolution to stellar explosions. The emphasis here was on experiments, and all of these examples pushed against various technological limitations. Progress in the areas of accelerators, detectors and techniques, which are important in other areas of nuclear physics, will continue to have a major impact here as well. It is also clear that in extreme stellar environments, where nucleosynthesis is governed by quasi-equilibria and by the global properties of the gas, the distinction between nuclear structure and nuclear astrophysics is blurred. Thus, the r-process can be approached in the context of astrophysics and/or as a venue for nuclear structure. The general areas described here will continue to be the frontier topics of nuclear astrophysics. Ultimately, nuclear astrophysics derives its motivation from astrophysical observations, whose continuing theme is serendipity. So surprising new results are to be expected.

This work was supported by the U.S. Department of Energy under contracts DE-AC05-76OR00033 and DE-FG02-97ER-41041. I would also like to thank the Boston Red Sox for proving me right (finally).

References

1. B. Chaboyer *et al.*, Astrophys. J. **494**, 96 (1998).
2. U. Schröder *et al.*, Nucl. Phys. A **467**, 240 (1987).
3. E.G. Adelberger *et al.*, Rev. Mod. Phys. **70**, 1265 (1998).
4. C. Angulo, P. Descouvemont, Nucl. Phys. A **690**, 755 (2001).
5. P.F. Bertone *et al.*, Phys. Rev. Lett. **87**, 152501 (2001).
6. A.M. Mukhamedzhanov *et al.*, Phys. Rev. C **67**, 065804 (2003).
7. K. Yamada, *et al.*, Phys. Lett. B **579**, 265 (2004).
8. A. Formicola *et al.*, Phys. Lett. B **591**, 61 (2004).
9. R.C. Runkle *et al.*, Phys. Rev. Lett. **94**, 082503 (2005).
10. C. Angulo, A.E. Champagne, H.P. Trautvetter, in *Proceedings of Nuclei in the Cosmos 8* (2004), to be published in Nucl. Phys. A.
11. C. Angulo *et al.*, Nucl. Phys. A **656**, 3 (1999).
12. G. Imbriani *et al.*, Astron. Astrophys. **420**, 625 (2004).
13. D.N. Spergel, *et al.*, Astrophys. J. Suppl. **148**, 175 (2003).
14. D. Bardayan *et al.*, Phys. Rev. Lett. **89**, 262501 (2002).
15. N. deSéréville *et al.*, Phys. Rev. C **67**, 052801(R) (2003).
16. R.L. Kozub *et al.*, Phys. Rev. C **71**, 032801 (2005).
17. J. José, A. Coc, M. Hernanz, Astrophys. J. **520**, 347 (1999).
18. C. Iliadis *et al.*, Astrophys. J. Suppl. **142**, 105 (2002).
19. S. Bishop *et al.*, Phys. Rev. Lett. **90**, 162501, 229902(E) (2003).
20. J.M. D'Auria *et al.*, Phys. Rev. C **69**, 065803 (2004).
21. H. Schatz *et al.*, Phys. Rev. Lett. **86**, 3471, (2001).
22. S.E. Woosley *et al.*, Astrophys. J. Suppl. **151**, 75 (2004).
23. J. Görres, M. Wiescher, F.-K. Thielemann, Phys. Rev. C **51**, 392 (1995).
24. H. Schatz *et al.*, Phys. Rep. **294**, 167 (1998).
25. J.A. Clark *et al.*, Phys. Rev. Lett. **92**, 192501, (2004); these proceedings.
26. B.A. Brown *et al.*, Phys. Rev. C **65**, 045802 (2002).
27. A. Wohr *et al.*, Nucl. Phys. A **742**, 349 (2004).
28. E. Bouchez *et al.*, Phys. Rev. Lett. **90**, 082502, (2003).
29. L. Nittler, Earth Planet. Sci. Lett. **209**, 259 (2003).
30. A.N. Nguyen, E. Zinner, Science **303**, 1496 (2004).
31. L.R. Nittler *et al.*, Astrophys. J. **483**, 475 (1997).
32. J.W. Truran *et al.*, Publ. Astron. Soc. Pac. **114**, 1293 (2002).
33. J.J. Cowan *et al.*, Astrophys. J. **521**, 194 (1999).
34. S. Wanajo *et al.*, Astrophys. J. **577**, 853 (2002).
35. K.-L. Kratz *et al.*, New Astron. Rev. **48**, 105 (2004).
36. F. Käppeler, H. Beer, K. Wisshak, Rep. Prog. Phys. **52**, 945 (1989).
37. B.S. Meyer, J.S. Brown, Astrophys. J. Suppl. **112**, 199 (1997).
38. J. Engel *et al.*, Phys. Rev. C **60**, 014302 (1999).
39. R. Surman, J. Engel, Phys. Rev. C **64**, 035801 (2001).
40. K.-L. Kratz *et al.*, Astrophys. J. **403**, 216 (1993).
41. I. Dillmann *et al.*, Phys. Rev Lett **91**, 162503 (2003); K.-L. Kratz *et al.*, these proceedings.